Spin-Imbalanced Quasi-Two-Dimensional Fermi Gases

W. Ong,[1,2] Chingyun Cheng,[1,2] I. Arakelyan,[1] and J. E. Thomas[1,*]
[1]Department of Physics, North Carolina State University, Raleigh, North Carolina 27695, USA
[2]Department of Physics, Duke University, Durham, North Carolina 27708, USA
(Received 24 December 2014; published 19 March 2015)

We measure the density profiles for a Fermi gas of ^{6}Li containing N_1 spin-up atoms and N_2 spin-down atoms, confined in a quasi-two-dimensional geometry. The spatial profiles are measured as a function of spin imbalance N_2/N_1 and interaction strength, which is controlled by means of a collisional (Feshbach) resonance. The measured cloud radii and central densities are in disagreement with mean-field Bardeen-Cooper-Schrieffer theory for a true two-dimensional system. We find that the data for normal-fluid mixtures are reasonably well fit by a simple two-dimensional polaron model of the free energy. Not predicted by the model is a phase transition to a spin-balanced central core, which is observed above a critical value of N_2/N_1. Our observations provide important benchmarks for predictions of the phase structure of quasi-two-dimensional Fermi gases.

DOI: 10.1103/PhysRevLett.114.110403 PACS numbers: 03.75.Ss

Layered strongly correlated systems play important roles in the quest for high temperature superconductors. In high-transition temperature copper oxide and organic compounds, electrons are confined in a quasi-two-dimensional geometry, creating complex, strongly interacting many-body systems, for which the phase diagrams are not well understood [1]. The basic underlying mechanism for superconductivity, the pairing of fermions, can be disrupted by an unequal number of pairing species when the Fermi surfaces of the two spin components are mismatched, leading to exotic superconductivity in which pairs acquire finite momentum [2]. Such spin-imbalanced Fermi mixtures also can contain polarons, quasiparticles formed by mobile impurities in a fermionic bath. Ultracold atomic Fermi gases provide a new platform for emulation of these systems, with precise experimental control [3–8].

Previous studies of pairing in spin-imbalanced three-dimensional (3D) [9–11] and one-dimensional (1D) [12] Fermi gases revealed phase separation. In 3D, a spin-balanced, fully paired, superfluid core is surrounded by an imbalanced normal-fluid shell, followed by a fully polarized shell, a structure successfully described by an elegant polaron model [13]. For measurements in 1D imbalanced mixtures, the behavior is reversed: A balanced phase appears outside a spin-imbalanced core, in agreement with a mean-field model.

A natural question is how the phase diagram of a quasi-two-dimensional cloud, containing a spin-imbalanced Fermi gas, differs from those measured in one and three dimensions. Does phase separation occur? If so, what separates? Unlike a 3D gas in free space, a two-dimensional (2D) gas naturally contains bound dimers [14,15]. The binding energy of these dimers, $E_b \geq 0$, sets the natural scale of length for scattering interactions in 2D systems. 2D polarons [16] may be important for a quasi-2D Fermi gas [17]. The phase diagram for imbalanced mixtures in this regime is therefore likely to be very rich [18–20], involving the interplay and phase separation of several components, including dimer gases, polaron gases, and spin-imbalanced normal fluids, as shown in Fig. 1. Exotic components with spatially modulated superfluids (Fulde-Ferrell-Larkin-Ovchinnikov states), and vortex-anti-vortex pairs (Berezinskii-Kosterlitz-Thouless states) also have been predicted for 2D and quasi-2D Fermi gases [19,21–27]. The dimensionality of a single layer in Fig. 1 is determined by the ratio of the transverse Fermi energy E_F to the energy level spacing $h\nu_z$ in the tightly confined z direction. The system is two dimensional if $E_F/h\nu_z \ll 1$ or three dimensional if $E_F/h\nu_z \gg 1$.

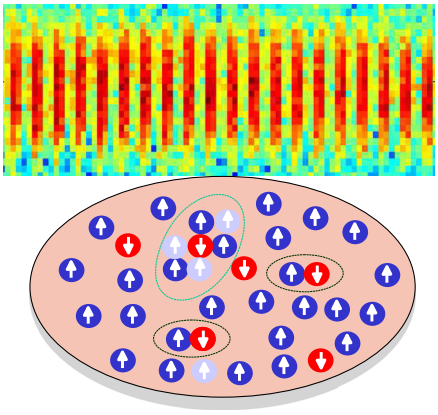

FIG. 1 (color online). Top: Side image of layered pancake-shaped atom clouds, separated by 5.3 μm in a CO_2 laser standing-wave trap. Bottom: In each pancake, confinement causes majority spins (blue-up arrow) and minority spins (red-down arrow) to pair, producing bound dimers. Polarons form when minority atoms scatter in the Fermi sea of the majority atoms and become surrounded by a cloud of particle-hole pairs (dark-blue-light-blue). Tightly bound dimers also scatter, forming dressed dimers.

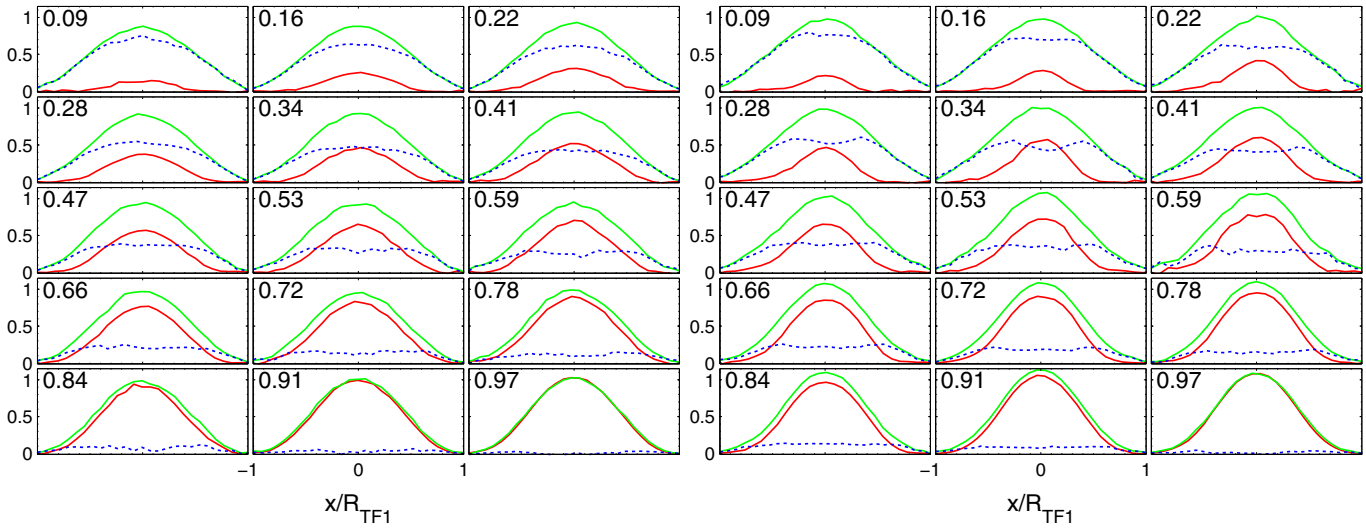

FIG. 2 (color online). Measured column density profiles in units of N_1/R_{TF1} at 832 G, for $E_F/E_b = 6.6$ (left panel) and at 775 G, for $E_F/E_b = 0.75$ (right panel) versus N_2/N_1. Green: 1-majority, red: 2-minority. Blue-dashed: Column density difference. Each profile is labeled by its N_2/N_1 bin (range ± 0.03). For the density difference, the flat center and two peaks at the edges are consistent with a fully paired core of the corresponding 2D density profiles. These features are more prominent for the higher interaction strength (right panel).

We report measurements of the spatial profiles for degenerate spin-imbalanced mixtures in the intermediate quasi-two-dimensional regime [17], where $E_F/(h\nu_z) \simeq 1$. This regime is of great interest, as the onset of a superfluid phase is predicted [20,28] to occur at a higher critical temperature than for a true 2D system. Control of the relative spin population permits precision studies of the phase diagram for these quasi-2D gases, which has been the topic of intense theoretical study [14,19–27,29].

In the experiments, typical parameters [30] are $N_1 = 800$ atoms per pancake trap at a temperature $T/T_F < 0.21$, trap potential depth $U_0 = 3.3\ \mu$K, harmonic oscillation frequencies $\omega_\perp = 2\pi \times 440$ Hz and $\omega_z = 2\pi \times 9.0$ kHz ($h\nu_z = 0.43\ \mu$K), $E_{F1} = 0.85\ \mu$K, Thomas-Fermi radius $R_{\mathrm{TF1}} = 17.5\ \mu$m; at 775 G, $E_b = 1.15\ \mu$K.

We investigate 2D density distributions $n_{2\mathrm{D}}(x, y)$ of imbalanced quasi-2D gases by direct imaging, which measures the column density profiles $n_{1\mathrm{D}}(x) = \int dy n_{2\mathrm{D}}(x, y)$, Fig. 2, as a function of E_F/E_b and N_2/N_1. Here $N_1(N_2)$ is the number of majority(minority) atoms. The cutoff radii R and the central 2D densities for each state are extracted using the fit function $n_{1\mathrm{D}}(x) = n_{1\mathrm{D}}(0)(1 - x^2/R^2)^{3/2}$, i.e., the y-integrated spatial profile of an ideal 2D Fermi gas [30]. Figure 3 shows the cloud radii for the majority (blue dots) and minority (red dots), for $E_F/E_b = 6.6, 2.2$, and 0.75. Both radii are given in units of

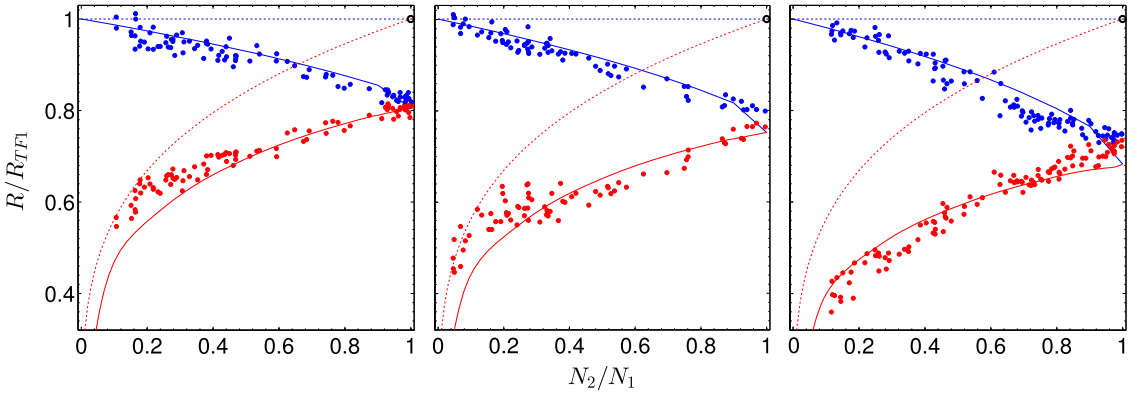

FIG. 3 (color online). Majority radii (upper-blue) and minority radii (lower-red) in units of the Thomas-Fermi radius for the majority for $E_F/E_b = 6.6$ (left panel), $E_F/E_b = 2.1$ (middle panel) and $E_F/E_b = 0.75$ (right panel). Dots: Data; solid lines: 2D polaron model for imbalanced mixture $0 \le N_2/N_1 \le 0.9$ [30], 2D polaron model for balanced mixture $N_2/N_1 = 1$ [30]. Dashed lines: Ideal Fermi gas prediction, black circle upper right: 2D-BCS theory for a balanced mixture.

the Thomas-Fermi radius R_{TF1} for the majority, to clearly demonstrate the deviation from the predictions for an ideal Fermi gas, which is shown for comparison as the blue-dashed and red-dashed curves. For the nearly polarized clouds, where $N_2/N_1 = 0.1$, the measured majority radii approach the ideal gas limit. As the N_2/N_1 is increased, the measured radii of both species are significantly affected by attractive interactions between the two spin components.

To consider many-body interactions, we first compare the measured cloud radii for the balanced mixture, $N_2/N_1 = 1$, with Bardeen-Cooper-Schrieffer (BCS) theory predictions for a true 2D Fermi gas [14], which shows $\epsilon_F = \mu + E_b/2$. This yields profiles identical to those of an ideal gas [30,39], leading to $R/R_{\mathrm{TF1}} = 1$ for both spin states (black circle, Fig. 3), in disagreement with the measured radii, which are much smaller.

Now we compare the data in Fig. 3 to a 2D polaron model, assuming, for simplicity, that most of the atoms reside in the ground axial state. The model is briefly summarized here and described in detail in the Supplemental Material [30]. At zero temperature, the free energy density f is equal to the energy density. For an imbalanced mixture, with $N_2 \ll N_1$, we assume the 2D energy density is

$$f = \frac{1}{2} n_1 \epsilon_{F1} + \frac{1}{2} n_2 \epsilon_{F2} + n_2 E_p(2). \tag{1}$$

Here, the first two terms are the energy density for a noninteracting gas and the last term is the energy density for minority polarons in state 2, which arises from scattering in the bath of majority atoms in state 1; $n_{1,2}$ and $\epsilon_{F1,2}$ are the corresponding densities and local Fermi energies. The two-polaron energy per particle $E_p(2) \equiv y_m(q_1)\epsilon_{F1}$, where $q_1 \equiv \epsilon_{F1}/E_b$. The function $y_m(q_1)$ is derived for a 2D gas in Ref. [17]. For simplicity, we use an analytic approximation [40], $y_m(q_1) = -2/\log(1 + 2q_1)$. From Eq. (1), we directly obtain the local chemical potentials, $\mu_1 = \partial f/\partial n_1$ and $\mu_2 = \partial f/\partial n_2$, and the corresponding local 2D pressure, $p = n_1\mu_1 + n_2\mu_2 - f$. The chemical potentials determine the spatial profiles in the trap.

The polaron model predictions for R_1 and R_2 are shown as the upper (blue) and lower (red) solid curves in Fig. 3. Although the model is strictly valid only for small N_2/N_1, we display the predictions based on Eq. (1) for the imbalanced gas for $N_2/N_1 = 0$ up to $N_2/N_1 = 0.9$. For $N_2/N_1 = 1$, we show the predictions for the balanced mixture, which employs a spin-symmetrized free energy density [30].

The central pressure for the balanced gas ($N_2 = N_1$) is determined by the 2D central density $n(0)$, which is directly obtained from the measured central column density $n_{1\mathrm{D}}(0)$. As discussed in the Supplemental Material [30], $p \propto 1/n(0)^2$ and $n(0) \propto n_{1\mathrm{D}}^2(0)/N_1$.

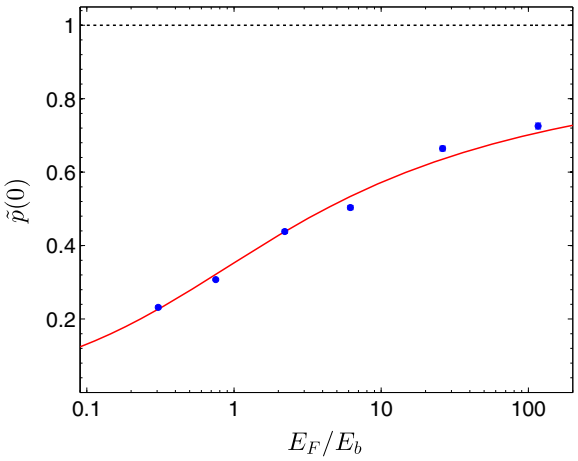

FIG. 4 (color online). Reduced 2D pressure at the trap center versus E_F/E_b for the balanced gas. Dots: Experiment, solid red curve: prediction based on the polaron model for the balanced gas, dashed line: prediction of 2D-BCS theory.

From this, we obtain the 2D pressure at the trap center in units of the ideal Fermi gas pressure for the same density, $\tilde{p}$, Fig. 4. The red solid curve shows the 2D polaron model prediction, for the same trap frequency $\omega_\perp$ as used to determine R_{TF1} in the cloud profile measurements, with no other adjustable parameters. For comparison, using the 2D-BCS theory prediction [14,39], where $\epsilon_F = \mu + E_b/2$, the Gibbs-Duhem relation requires $\tilde{p} = 1$ for all E_F/E_b, in contrast to the measurements [30].

We have also measured the central density ratio n_2/n_1 of the 2D gas as a function of N_2/N_1. First, we fit a Thomas-Fermi 1D profile to each column density, from which we find the corresponding 2D densities as described above. Also, we employ an inverse Abel transformation of the column densities to extract the peak 2D densities. Both methods yield similar results within 5%. We show the density ratios for three interaction strengths in Fig. 5. The agreement with the polaron model is reasonably good at 832 G, where $E_F/E_b = 6.6$. However, as the interaction strength is increased to $E_F/E_b = 0.75$ by increasing the dimer binding energy at 775 G, the 2D central densities abruptly become balanced above a critical ratio N_2/N_1 (right panel, Fig. 5). To ensure that the densities are balanced not just at the center, but over an extended range, we examine the measured column density profiles in Fig. 2. The apparent presence of two peaks at the edges in the column density difference versus x is consistent with the y-integrated 2D shell structure of a balanced core surrounded by an unpaired majority fraction [30]. Note that double integration of the 3D shell structure gives rise to flat top distributions [41].

Equal densities for any imbalance are not predicted by the 2D polaron model, as the pressure determined for the imbalanced gas from Eq. (1) is always greater than or equal

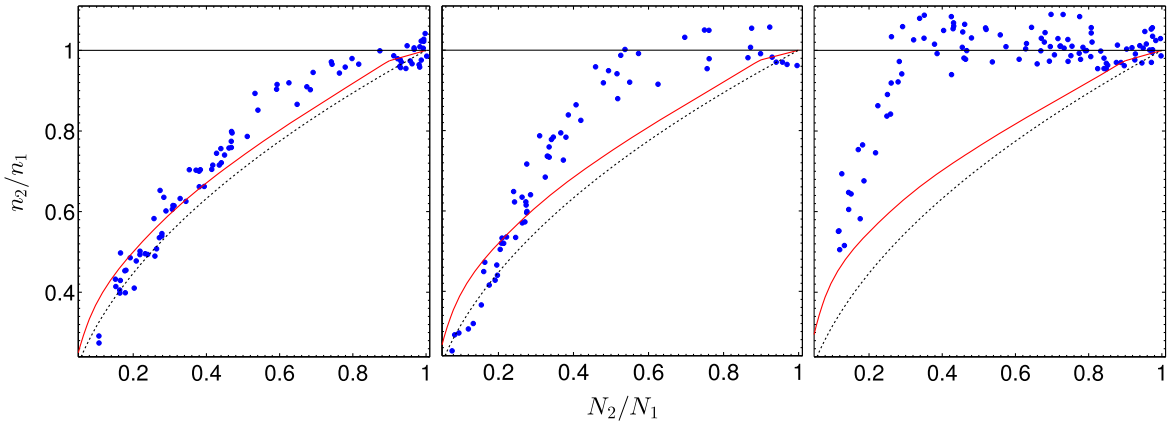

FIG. 5 (color online). Ratio of minority to majority 2D central densities for $E_F/E_b = 6.6$ (left panel), $E_F/E_b = 2.1$ (middle panel), and for the strongest interactions $E_F/E_b = 0.75$ (right panel). Blue dots: data, red solid line: 2D polaron model, dashed black line: ideal Fermi gas prediction. Stronger interactions balance the central densities over an extended range of imbalance, in clear disagreement with the polaron model.

to the pressure for the balanced gas, contrary to the 3D case where crossing of the two pressures determines the critical polarization for the phase separation [13]. This is not unexpected, as the simple polaron model with the analytic approximation for the polaron energy ignores nonmonotonic behavior [42] on the molecular side of the Feshbach resonance ($B < 832$ G), where it overestimates the magnitude of E_p and does not include the effective mass or molecular repulsion energy. Further, the polaron model is derived for zero temperature and considers only the ground axial state of motion in the trap. However, for the experiments, we estimate the upper limit of the gas temperature to be $k_B T/E_F = 0.21$, and a population of the first excited axial state up to 20% for a noninteracting gas [30]. For interacting mixtures, dimer pairing decreases the local Fermi energy of both components, suppressing the population of higher axial states, which can be included in more complete treatments.

In conclusion, we have created and studied an imbalanced strongly interacting quasi-two-dimensional Fermi gas. The 2D polaron model captures much of the behavior of the spin-imbalanced normal-fluid mixtures, suggesting that polarons play an important role. However, more precise calculations of the pressures for the balanced and imbalanced components are needed to explain the observed phase separation and critical spin imbalance. Our measurements will serve as a test for predicted phase diagrams, which will help to reveal the structure of a quasi-2D Fermi gas.

This research is supported by the Physics Division of the Army Research Office (many-body physics in two-dimensional Fermi gases), and the Division of Materials Science and Engineering, the Office of Basic Energy Sciences, Office of Science, U.S. Department of Energy (thermodynamics in strongly correlated Fermi gases). Additional support has been provided by the Physics Divisions of the National Science Foundation and the Air Force Office of Scientific Research. We thank M. Bluhm, T. Schäfer, and D. Lee, North Carolina State University, for stimulating conversations.

*Corresponding author.
jethoma7@ncsu.edu

[1] M. R. Norman, Science **332**, 196 (2011).
[2] H. Mayaffre, S. Kramer, M. Horvatic, C. Berthier, K. Miyagawa, K. Kanoda, and V. F. Mitrovic, Nat. Phys. **10**, 928 (2014).
[3] A. Schirotzek, C.-H. Wu, A. Sommer, and M. W. Zwierlein, Phys. Rev. Lett. **102**, 230402 (2009).
[4] K. Martiyanov, V. Makhalov, and A. Turlapov, Phys. Rev. Lett. **105**, 030404 (2010).
[5] M. Feld, B. Frohlich, E. Vogt, M. Koschorreck, and M. Kohl, Nature (London) **480**, 75 (2011).
[6] A. T. Sommer, L. W. Cheuk, M. J. H. Ku, W. S. Bakr, and M. W. Zwierlein, Phys. Rev. Lett. **108**, 045302 (2012).
[7] M. Koschorreck, D. Pertot, E. Vogt, B. Frohlich, M. Feld, and M. Kohl, Nature (London) **485**, 619 (2012).
[8] M. G. Ries, A. N. Wenz, G. Zürn, L. Bayha, I. Boettcher, D. Kedar, P. A. Murthy, M. Neidig, T. Lompe, and S. Jochim, arXiv:1409.5373v1.
[9] M. W. Zwierlein, A. Schirotzek, C. H. Schunck, and W. Ketterle, Science **311**, 492 (2006).
[10] G. B. Partridge, W. Li, R. I. Kamar, Y.-a. Liao, and R. G. Hulet, Science **311**, 503 (2006).
[11] Y. i. Shin, C. H. Schunck, A. Schirotzek, and W. Ketterle, Nature (London) **451**, 689 (2008).
[12] Y.-a. Liao, A. S. C. Rittner, T. Paprotta, W. Li, G. B. Partridge, R. G. Hulet, S. K. Baur, and E. J. Mueller, Nature (London) **467**, 567 (2010).
[13] F. Chevy and C. Mora, Rep. Prog. Phys. **73**, 112401 (2010).
[14] M. Randeria, J.-M. Duan, and L.-Y. Shieh, Phys. Rev. Lett. **62**, 981 (1989).

[15] D. S. Petrov and G. V. Shlyapnikov, Phys. Rev. A **64**, 012706 (2001).
[16] S. Zöllner, G. M. Bruun, and C. J. Pethick, Phys. Rev. A **83**, 021603 (2011).
[17] Y. Zhang, W. Ong, I. Arakelyan, and J. E. Thomas, Phys. Rev. Lett. **108**, 235302 (2012).
[18] H. Caldas, A. L. Mota, R. L. S. Farias, and L. A. Souza, J. Stat. Mech. (2012) P10019.
[19] S. Yin, J.-P. Martikainen, and P. Törmä, Phys. Rev. B **89**, 014507 (2014).
[20] A. M. Fischer and M. M. Parish, Phys. Rev. B **90**, 214503 (2014).
[21] J.-P. Martikainen and P. Törmä, Phys. Rev. Lett. **95**, 170407 (2005).
[22] S. S. Botelho and C. A. R. Sá de Melo, Phys. Rev. Lett. **96**, 040404 (2006).
[23] W. Zhang, G.-D. Lin, and L.-M. Duan, Phys. Rev. A **78**, 043617 (2008).
[24] J. Tempere, S. N. Klimin, and J. T. Devreese, Phys. Rev. A **79**, 053637 (2009).
[25] G. Bertaina and S. Giorgini, Phys. Rev. Lett. **106**, 110403 (2011).
[26] M. Bauer, M. M. Parish, and T. Enss, Phys. Rev. Lett. **112**, 135302 (2014).
[27] D. E. Sheehy, arXiv:1407.8021v1.
[28] M. Baranov, D. Efremov, and M. Kagan, Physica (Amsterdam) **218C**, 75 (1993).
[29] J. Kinnunen, L. M. Jensen, and P. Törmä, Phys. Rev. Lett. **96**, 110403 (2006).
[30] See Supplemental Material at http://link.aps.org/supplemental/10.1103/PhysRevLett.114.110403 for details of the experimental setup, thermometry, and predictions of the 2D polaron model, which includes Refs. [31–38] .
[31] A. A. Orel, P. Dyke, M. Delehaye, C. J. Vale, and H. Hu, New J. Phys. **13**, 113032 (2011).
[32] V. Makhalov, K. Martiyanov, and A. Turlapov, Phys. Rev. Lett. **112**, 045301 (2014).
[33] K. M. O'Hara, S. L. Hemmer, M. E. Gehm, S. R. Granade, and J. E. Thomas, Science **298**, 2179 (2002).
[34] J. Kinast, A. Turlapov, J. E. Thomas, Q. Chen, J. Stajic, and K. Levin, Science **307**, 1296 (2005).
[35] M. Randeria and E. Taylor, Annu. Rev. Condens. Matter Phys. **5**, 209 (2014).
[36] F. Chevy, Phys. Rev. A **74**, 063628 (2006).
[37] Y.-i. Shin, Phys. Rev. A **77**, 041603 (2008).
[38] J. Levinsen and S. K. Baur, Phys. Rev. A **86**, 041602 (2012).
[39] L. He and P. Zhuang, Phys. Rev. A **78**, 033613 (2008).
[40] M. Klawunn and A. Recati, Phys. Rev. A **84**, 033607 (2011).
[41] Y. Shin, M. W. Zwierlein, C. H. Schunck, A. Schirotzek, and W. Ketterle, Phys. Rev. Lett. **97**, 030401 (2006).
[42] M. M. Parish and J. Levinsen, Phys. Rev. A **87**, 033616 (2013).